Nanoscale

Accepted Manuscript

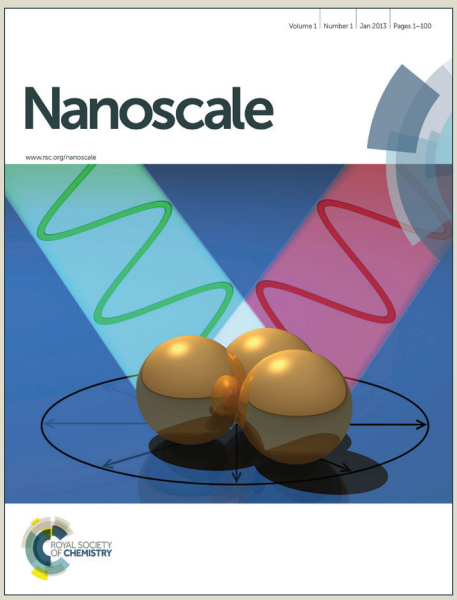

ROYAL SOCIETY OF CHEMISTRY

www.rsc.org/nanoscale

Real-time analysis of diaquat dibromide monohydrate in water with a SERS-based integrated microdroplet sensor

Rongke Gao,[a] Namhyun Choi,[a] Soo-Ik Chang,[b] Eun Kyu Lee[a] and Jaebum Choo*[a]

[a]*Department of Bionano Technology , Hanyang University, Ansan 426-791, South Korea*

[b]*Department of Biochemistry, Chungbuk National University, Cheongjoo 361-763, South Korea*

Submitted to

Nanoscale (Second Revision)

May 2014

Type of Manuscript: Research Paper

***Corresponding author**

Address for correspondence:

Jaebum Choo

Telephone: +82-31-400-5201; Fax: +82-31-436-8188; E-mail: jbchoo@hanyang.ac.kr

Abstract

We report the fast and sensitive trace analysis of diaquat dibromide monohydrate (DQ) in water using a surface-enhanced Raman scattering (SERS)-based microdroplet sensor. This sensor is composed of two compartments, the first being for droplet generation for fresh silver nanoparticle (AgNP) synthesis, and the second for droplet merging for SERS detection. Silver ions were nucleated and grown to large size AgNPs in droplets, and then each droplet was synchronously merged with another droplet containing DQ for SERS detection. This two-phase liquid-liquid segmented flow system prevented memory effects caused by the precipitation of nanoparticle aggregates on channel walls because the aqueous droplets were isolated by a continuous oil phase. The limit of detection (LOD) of DQ in water was determined to be below 5 nM, which satisfies the maximum contaminant level defined by the United States EPA. This method was also validated successfully in DQ-spiked tap water. The SERS-based integrated sensing system is expected to be useful as an in-the-field sensing platform for fast and reproducible trace analysis of environmental pollutants in water.

1. Introduction

In the past decade, microfluidic chips have been extensively used for the highly controlled synthesis of colloidal nanoparticles.[1-3] Compared to conventional macro-scale batch synthesis, miniaturization of such systems using microfluidic technology offers significant advantages including precise control, high throughput, high speed, and reproducibility due to improved heat and mass transfer effects as a result of system downscaling.[4,5] Continuous flow-based microfluidic chips have been used previously for on-chip synthesis of earlier stage colloidal nanoparticles.[6-8] However, the associated "memory effect" is a serious problem in the continuous flow regime because it causes the deposition of particle aggregates on the walls of microfluidic channels.[9-11] Fortunately, this problem can be avoided by switching from a continuous flow to a segmented flow regime. Here, segmented flow is induced by introducing an additional immiscible fluid into the channel, causing the reaction phase to divide into a succession of discrete droplets. The two-phase liquid-liquid segmented flow system prevented the aggregation of nanoparticles on the channel walls due to localization of reagents within encapsulated droplets, which reduced residence time distributions. The use of segmented flow has been recently applied to the synthesis of many different types of nanoparticles.[12-15]

An additional issue of similar importance in droplet-based microfluidic systems is the on-line characterization of droplets at high flow speed and low analyte concentration. Indeed, a real-time detection technique with high sensitivity is necessary to collect chemical or biological information from droplet-based microfluidic systems. To date, a number of detection methods, including time-resolved fluorescence spectroscopy,[16,17] fluorescence polarization,[18] fluorescence resonance energy transfer (FRET),[19] fluorescence life-time

imaging,[20,21] Raman spectroscopy,[22-24] and electrochemical detection methods,[25,26] have been used for the characterization of multiple droplets. However, the labeling of fluorescence tags and photo-bleaching effects in fluorescence detection and the low sensitivity issue in electrochemical detection remain obstacles for real-time characterization of droplets. Recently, surface-enhanced Raman scattering (SERS)-based detection techniques have been considered as a promising alternative for highly sensitive detection of multiple droplets.[27,28] When analyte molecules are adsorbed onto roughened metal surfaces, the associated SERS signals are greatly increased due to electromagnetic and chemical enhancements at SERS active sites known as "hot spots" upon exposure to an excitation laser source. This enhancement shows promise in overcoming the low sensitivity problem inherent in conventional Raman, fluorescence, and electrochemical detection. We have previously demonstrated that the combination of a microdroplet system with SERS detection is a powerful analytical tool for fast and reproducible trace analysis of environmental pollutants such as mercury (II) ions[29] and paraquat[30] in water. In our previous works, silver nanoparticles were synthesized under batch conditions and injected into a droplet channel together with target analytes for SERS detection. However, performing particle synthesis in a microdroplet system provides a higher level of reaction control as well as an automatic synthetic process. Consequently, fabrication of freshly synthesized silver nanoparticle seeds with tunable growth is possible under droplet flow conditions. In addition, a sequential droplet merging process between an aqueous droplet containing AgNPs and another droplet containing target analytes is also needed for the adsorption of analytes on the surface of AgNPs. For this purpose, we implemented both of these functions (AgNPs synthesis and droplet merging and detection) in a single microdroplet channel.

Diquat dibromide monohydrate (DQ) was selected as a target analyte for the SERS-based microdroplet sensor. DQ is a fast-acting and non-selective herbicide widely used in agriculture to control broadleaf and grassy weeds. However, DQ is also known to be highly toxic to humans, and the specific toxic effects of DQ on human organs have been investigated in patients who died as a result of DQ poisoning.[31,32] With respect to drinking water, the U.S. Environmental Protection Agency (EPA) has established a maximum contaminant level of 60 nM for DQ.[33] Nonetheless, analysis of DQ remains complicated because its ionic nature makes it difficult for DQ to be retained by standard reverse phase HPLC. Accordingly, there is still an urgent need to develop a fast, sensitive, and reliable detection method for trace analysis of DQ in drinking water.

Herein, we report a conceptually new integrated microfluidic system composed of two different segmented flow regimes, the first being a microdroplet channel for the synthesis of fresh silver nanoparticles, and the other a merging channel between AgNPs and DQs to allow for SERS detection. To the best of our knowledge, this is the first report of highly sensitive trace analysis of DQ using a continuous on-line SERS-based integrated microdroplet sensor.

2. Experimental

2.1. Materials

Silver nitrate (99%), hydroxylamine hydrochloride (98%), 1H,1H,2H,2H-perfluorooctanol (PFO, 97%), diquat dibromide monohydrate (DQ, 99.5%), trichloro(1H,1H,2H,2H-perfluorooctyl)silane (97%), potassium bromide (99%), and sodium hydroxide (99.5%) were purchased from Sigma–Aldrich. Absolute ethanol (99.9%) was

purchased from Merck. Polydimethylsiloxane (PDMS, Sylgard 184 Silicone. Elastomer Kit) was purchased from Dow Corning. FC-40 (a mixture of perfluoro-tri-n-butylamine and perfluoro-di-nbutylmethylamine) and FC-70 (perfluorotripentylamine) were obtained from 3M. Deionized water was purified by a Milli-Q water purification system (Millipore Corporation, Billerica, MA, USA).

2.2. Fabrication of the microfluidic device

A positive SU-8 photoresist mold was fabricated using a standard soft lithographic technique. PDMS prepolymer and curing agent (Sylgrad 184, Dow Corning) were mixed in a ratio of 10:1 w/w, degassed, and decanted into a positive mold. The resulting structure was cured at 70 ◦C for 2 h in an oven, and the structured layer was peeled from the mold. After punching inlet and outlet holes for fluidic access, the structured PDMS substrate was bonded to a thin cover glass using oxygen plasma. For hydrophobic treatments of the interior channel surface, the inside of the channel was filled with 2% (v/v) trichloro(1H,1H,2H,2H-perfluorooctyl)silane in FC-40 solution, immediately after which the entire device was placed in a desiccator for 1 h. The channel was then washed with ethanol and dried at 70 ◦C for 1 h to remove any remaining ethanol. The main channel and side channels were 200 μm and 100 μm wide, respectively. The depth of all other channels was 100 μm. A 10:20:3 (v/v) mixture of FC-40, FC-70, and 1H,1H,2H,2H-perfluorooctanol (PFO) was used as a carrier oil in this work.

2.3. Synthesis of silver nanoparticles

AgNPs were prepared through two different methods. The first method consisted of

conventional batch synthesis, while the second method consisted of on-chip synthesis. In both cases, AgNPs were synthesized using the method reported by Leopold and Lendl. The advantages of hydroxylamine hydrochloride-reduced silver colloids include fast preparation at room temperature and immediate applicability for SERS detection. In the batch synthesis, 1 mL of 0.25 M hydroxylamine hydrochloride was dissolved in 88 mL of deionized water, to which 1 mL of 0.3 M sodium hydroxide was added to maintain an alkaline pH. Secondly, 10 mL of 1.0×10^{-2} M silver nitrate was added dropwise to the solution with vigorous stirring. Finally, the solution was continuously stirred for an additional 2 h.

For on-chip synthesis of AuNPs, carrier oil, silver nitrate solution (3.3 mM), water, and hydroxylamine hydrochloride/sodium hydroxide solution (3.3 mM/6.7 mM) were preloaded in 1 mL Norm-Ject plastic syringes. The components were then injected into the microdroplet channels *via* tygon tubes connected to the punch holes. The flow rates of carrier oil and other aqueous solutions were controlled by precision syringe pumps and varied between 0.1 and 5.0 μL min^{-1}.

2.4. Droplet merging measurement and on-chip SERS detection

An Olympus IX71 inverted fluorescence microscope (Olympus Co., Japan) equipped with a high-speed camera (PCO AG, Germany) was employed for recording microdroplet merging and measuring droplet velocity. Precision syringe pumps (PHD 2000, Harvard Apparatus, USA), 1 mL Norm-Ject plastic syringes (Henke-Sass Wolf GmbH, Germany), a 32 mm-22 G needle (KOVAX-NEEDLE®, Korea Vaccine Co., Ltd., Seoul, Korea), and Tygon microbore tubing (ID=0.02 IN, Saint-Gobain PPL Corp.) were used to inject samples into the microdroplet channel.

SERS signals of DQ in the microdroplet channels were collected using a confocal Raman microscope system built in-house. The system consisted of an Innova 70 argon/krypton ion laser (Coherent Inc., USA), an Acton SP2500 monochrometer with a PIXIS charge-coupled device (CCD) camera (Princeton Instruments, USA), and an Olympus IX71 inverted microscope system (Olympus Co., Japan). The laser, operating at λ= 514.5 nm, was used as the excitation source with a power of approximately 6 mW. A 40× objective lens was used to focus the laser. The Rayleigh line was removed from the Raman scattering using a holographic notch filter in the collection path. Raman scattering was collected using a PIXIS CCD camera at a spectral resolution of 1 cm^{-1}.

All spectral manipulations were performed using GRAM/32 software from Galactic Industries Corporation. The measured Raman spectra contain two different types of spectral noise; one is the additive noise from external conditions and the other is a background noise from auto-fluorescence. These noises should be carefully treated because they strongly affect the quantitative analysis of DQ. A Savitzky-Golay filter was utilized to suppress additive noise because it is effective for preserving line width. On the other hand, two different methods were considered for the suppression of background noise; one is a smoothing derivative and the other is a linear programming. The smoothing derivative method includes frequency noise removal, estimation of the background derivative, interpolation and background elimination while the linear programming method adopts a polynomial as an approximating function.

Scanning electron microscope (SEM) images of AgNPs were obtained using a Tescan MIRA3 scanning electron microscope (Tescan USA, Inc.). AgNPs samples (10 μl) were dropped onto a slide glass and dried at room temperature for SEM measurement. UV/Vis

absorption spectra were recorded using a Cary 100 spectrophotometer (Varian, USA) with disposable polyacryl cuvettes.

3. Results and discussion

3.1. Design and fabrication of the integrated microdroplet channel

Figure 1(a) displays the schematic design of the PDMS microdroplet channel used in this study. The channel consisted of two compartments, the first being for synthesis of fresh silver nanoparticles, and the second for microdroplet merging and SERS detection. As shown in Fig. 1(b), the first compartment was composed of multiple winding channels (for high mixing efficiency) and a long diffusion channel (for fast growth of silver nucleation). The second compartment consisted of an intersection for merging of the two droplet streams and SERS detection, as shown in Fig. 1(c). Figure 1(d) displays a photograph of the microdroplet channel filled with two different colors (red and blue) of ink.

In the first compartment, a high mixing efficiency among silver nitrate solution, distilled water, and hydroxylamine hydrochloride/sodium hydroxide solutions was achieved in each droplet. Injecting the dispersed aqueous phase stream perpendicular to the continuous oil stream formed the droplets necessary to initiate AgNP synthesis. Droplet formation resulted from induced shear forces at the interface between the two different phases. After formation of droplets, aqueous samples in each droplet were mixed by transport through the winding channels. Synthesizing AgNPs within droplets separated by an immiscible fluid environment allowed for easy isolation of the reactants from the surrounding environment, thus avoiding contamination.

As shown in Fig. 1(a), AgNPs were prepared by the method reported by Leopold and

Lendl.[34] The advantages of hydroxylamine hydrochloride-reduced silver colloid include its fast preparation at room temperature and its immediate applicability for SERS. Here, sodium hydroxide was used to maintain the pH of the solution at basic conditions. The reaction between silver nitrate and hydroxylamine hydrochloride induced nucleation of silver ions, which gradually grew to larger AgNPs while passing through the long diffusion channel. In Fig. S1 (in ESI†), the quality of the on-chip synthesized silver colloids (a) was compared to that of conventional batch-synthesized colloids (b). SEM images of the batch-synthesized AgNPs and on-chip synthesized AgNPs displayed a distinct difference in morphology. Specifically, the batch-synthesized AgNPs exhibited a spherical morphology, while on-chip-synthesized AgNPs showed a cubic morphology. UV/Vis absorption spectra shown in Fig. S1(c) revealed similar absorption maxima for both AgNPs, although the on-chip-synthesized AgNPs showed a slightly more narrow absorption band pattern. The particle shapes and absorption band patterns of AgNPs formed by on-chip synthesis were consistent with previous results of AgNPs synthesized by continuous flow regimes.[27] However, it is noteworthy that the SERS signal of 5×10^{-6} M DQ for on-chip-synthesized AgNPs was much stronger than for batch-synthesized AgNPs, as shown in Fig. S1(d). Importantly, the reaction conditions could be readily tuned by varying the ratio of individual flow rates (to change the reaction stoichiometry), and thus the newly designed system provided excellent control of the final products synthesized on-chip.

3.2. Merging two droplets containing AgNPs and DQs

To validate the SERS effect on AgNP colloids, SERS spectra were measured for three different channel positions, as shown in Fig. 2(a). Here, laser light was focused on the carrier

oil (i), 2×10^{-5} M DQ solution (ii), and DQ adsorbed onto AgNPs (iii), respectively, and the corresponding SERS spectra are shown in Fig. 2(b). Raman signals of the 2×10^{-5} M DQ solution were detected only when DQ molecules were adsorbed onto AgNPs. In the respective cases of carrier oil and the DQ solution itself, only Raman signals from the PDMS polymer (1120 cm^{-1} and 1410 cm^{-1}) were observed. Based on these results, we concluded that the SERS technique was applicable for trace analysis of DQ. In addition, the Raman spectrum of carrier oil was measured to investigate its signal contributions (Fig. S2). As shown in this figure, the signal intensities for carrier oil are much weaker than that measured from DQ adsorbed AgNPs. In addition, the SERS peak centered at 1579 cm^{-1}, which was used for quantitative evaluation of DQ, was not overlapped with the ones of oil or PDMS. Consequently, the SERS signals from PDMS and carrier oil do not take an effect on the quantitative analysis of DQ.

Figure 3(a) shows the sequential merging mechanism between two droplets; the first is an AgNP droplet formed by the first droplet compartment, and the second is a droplet of DQ analytes coming from a secondary inlet. Inspection of Fig. 3(a) demonstrated that droplet merging was highly efficient at combining the two droplets to form a droplet twice as large. In addition, the droplet merging process was highly stable and could be operated continuously for periods of several hours. In these experiments, the flow rate of DQ droplets was controlled to generate optimal droplet margining in the winding channel.

In order to investigate the mixing efficiency of the microdroplet, SERS spectra were measured for 5×10^{-6} M DQ along the channel. Figure 3(a) shows six different channel positions for SERS measurement. Flow rates for carrier oil and aqueous streams were varied

between 0.1 and 5.0 μL min^{-1}. The optimal flow rates were determined to be 4.0 and 1.0 μL min^{-1} for the carrier oil and aqueous streams, respectively, and the volume of microdroplets was estimated to be 8 nL. After droplet formation, aqueous samples in each droplet were mixed by transport through the winding channels. The winding structures induced chaotic advections within each droplet, thus allowing extremely rapid and efficient mixing. To prevent the exposure of precursor solutions to light, syringes including precursor solutions were wrapped with aluminum foil.

SERS spectra at each channel position were collected for 30 s, which encompassed the transit of approximately 240 droplets (8 Hz) through the detection position. The merging process for all the droplets was observed using the high speed camera (Fig. S3), and confirmed that they were merged exactly one by one. In Fig. 3(b), the SERS spectrum of DQ was recorded at 1579 cm^{-1}, and its intensity was gradually increased along the channel. On the basis of a peak intensity at 1579 cm^{-1}, we estimated that DQ adsorption on AgNPs was approximately 80% complete at point 3. Figure 3 also shows that the adsorption was estimated to be almost complete by point 4, indicating the excellent mixing performance by transport through the winding structure in the microdroplet chip.

3.3. Quantitative analysis of DQ using on-line SERS detection

For evaluation of SERS detection performance, quantitative analysis of DQ was performed on two different types of AgNPs. Figure S4 compares the SERS response of DQ using on-chip-synthesized AgNPs with the same response using AgNPs synthesized off-chip under droplet flowing conditions. The SERS peak of DQ centered at 1579 cm^{-1}, assigned as the CN stretching mode, was used for quantitative evaluation of DQ. Other SERS peaks for

DQ were assigned on the basis of previously reported papers (Fig. S5 and Table S1).[35,36] In the case of on-chip AgNP synthesis, a dynamic range was constructed from 10^{-5} ~ 10^{-10} g/mL (from 11 different DQ concentration data points), as shown in Fig. S4(a). On the other hand, a dynamic range of 10^{-3} ~ 10^{-7} g/mL (from 7 data points) was found for batch-synthesized AgNPs, as shown in Fig. S4(b). These results indicated that on-chip-synthesized AgNPs had higher sensitivity and a wider detection range than batch-synthesized AgNPs.

Figure 4(a) illustrates the SERS spectra for different concentrations of DQ at position 6 in Fig. 3(a). The resulting calibration curve in the linear range (5×10^{-6} ~5×10^{-9} g/mL) is shown in Fig. 4(b). The SERS signal intensity increased concomitantly with increasing DQ concentration, which can be used for quantitative determination of DQ in drinking water. The limit of detection (LOD) assessed from the standard deviations from three measurements was estimated to be 5×10^{-9} M and had a correlation coefficient of 0.995. This SERS-based microdroplet sensor was also validated for drinking tap water. Four different concentrations of DQ (5×10^{-6}~5×10^{-9} M) were spiked into a tap water. Figure S6 illustrates the SERS spectra and corresponding calibration curve. As shown in this figure, a good linear response was also found for the spiked tap water. All the experiments were performed in the two-phase liquid/liquid segmented flow system (microdroplet channel). Finally, the SERS measurements were also repeated for three different chips to investigate the chip-to-chip reproducibility. As shown in Fig. S7, no SERS intensity variation was found for different chips when the measurement was carried out under the same condition. To further investigate the reliability of the data, we performed 50 SERS measurements for each microdroplet chip. On the basis of the measured spectral data, their mean SERS spectra of DQ (solid lines) together with the respective double standard deviations (blue tubes) for three chips[37,38] were

displayed in Fig. S8. Here, average standard deviations for three chips were calculated to be 0.117, 0.112, and 0.115, respectively. Since those values are significantly small, it can be concluded that these dataset is statistically reliable, and the chip-to-chip reproducibility is acceptable for different measurements. Taken together, our experimental data demonstrated that the on-line SERS-based microdroplet sensor employing fresh on-chip-synthesized AgNPs is a very sensitive analytical technique for real-time trace analysis of DQ in drinking water.

4. Conclusions

In the present study, we fabricated a novel integrated microdroplet sensor for real-time analysis of DQ in drinking water. This sensor is composed of two droplet compartments, one for the on-chip synthesis of fresh AgNPs, and the other for droplet merging and SERS detection. Silver ions were nucleated and grown to larger size silver nanoparticles in droplets, and then each droplet was synchronously merged with a droplet containing DQ analytes for SERS detection. A LOD of 5 nM is possible using this SERS-based microdroplet sensor, which satisfies the maximum contaminant level defined by the United States EPA. This method was also validated successfully for DQ-spiked tap water. In addition, fast and reproducible quantitative analysis with a tiny volume of sample was possible because all of the detection processes were automatically performed in the specially designed microdroplet sensor. Thus, this miniaturized and integrated SERS-based microdroplet sensor may be readily used as an in-the-field sensing platform. Finally, the combination of droplet merging system with in situ AgNPs synthesis for on-line SERS detection is expected to be a powerful analytical tool for the fast and reproducible trace analysis of environmental pollutants in

drinking water.

Acknowledgements

The National Research Foundation of Korea supported this work through grant numbers R11-2008-0061852, K20904000004-13A0500-00410. We also acknowledge financial support from the BioNano Health-Guard Research Center funded by the Ministry of Science, ICT & Future Planning of Korea as the Global Frontier Project (grant number 2013M3A6B2078957). This study was also partially supported by a grant of the Korean Health Technology R&D Project, Ministry of Health & Welfare, Republic of Korea through grant number A121983.

References

1. A. M. Nightingale and J. C. deMello, Adv. Mater., 2013, 25, 1813-1821.
2. A. J. deMello, Nature, 2006, 442, 394-402.
3. E. M. Chan, R. A. Mathies and A. P. Alivisatos, Nano Lett., 2003, 3, 199-201.
4. A. M. Nightingale and J. C. deMello, J. Mater. Chem., 2010, 20, 8454-8463.
5. L. H. Hung, K. M. Choi, W. Y. Tseng, Y. C. Tan, K. J. Shea and A. P. Lee, Lab Chip, 2006, 6, 174-178.
6. Z. L. Xue, A. D. Terepka and Y. Hong, Nano Lett., 2004, 4, 2227-2232.
7. H. Nakamura, A. Tashiro, Y. Yamaguchi, M. Miyazaki, T. Watari, H. Shimizu and H. Maeda, Lab Chip, 2004, 4, 237-240.
8. J. B. Edel, R. Fortt, J. C. deMello and A. J. deMello, Chem. Commun., 2002, 1136-1137.
9. K. R. Strehle, D. Cialla, P. Rosch, T. Henkel, M. Kohler, J. Popp, Anal. Chem., 2007, 79, 1542-1547.
10. K. R. Ackermann, T. Henkel, J. Popp, Chem. Phys. Chem., 2007, 8, 2665-2670.
11. H. Song, J. D. Tice and R. F. Ismagilov, Angew. Chem. Int. Ed., 2003, 42, 767-772.
12. P. H. Hoang, H. Park and D. P. Kim, J. Am. Chem. Soc., 2011, 133, 14765-14770.
13. E. M. Chan, A. P. Alivisatos and R. A. Mathies, J. Am. Chem. Soc., 2005, 127, 13854-13861.
14. A. M. Nightingale, S. H. Krishnadasan, D. Berhanu, X. Niu, C. Drury, R. McIntyre, E. Valsami-Jones and J. C. deMello, Lab Chip, 2011, 11, 1221-1227.
15. J. Wagner and J. M. Kohler, Nano Lett., 2004, 4, 2227-2232.
16. S. L. Sjostrom, H. N. Joensson and H. A. Svahn, Lab Chip, 2013, 13, 1754-1761.
17. X. Casadevall i Solvas, M. Srisa-Art, A. J. deMello and J. B. Edel, Anal. Chem., 2010, 82, 3950-3956.
18. J. W. Choi, D. K. Kang, H. Park, A. J. deMello and S. I. Chang, Anal. Chem., 2012, 17, 3849-3854.
19. M. Srisa-Art, J. deMello and J. B. Edel, Anal. Chem., 2007, 79, 6682-6689.
20. A. N. Rao, N. Vandencasteele, L. J. Gamble and D. W. Grainger, Anal. Chem., 2012, 84, 10628-10636.

21. M. Srisa-Art, A. J. deMello and J. B. Edel, Phys. Rev. Lett., 2008, 101, 014502/1-014502/4.
22. M. P. Cecchini, J. Hong, C. Lim, J. Choo, T. Albrecht, A. J. deMello and J. B. Edel, Anal. Chem., 2011, 83, 3076-3081.
23. E. Chung, R. Gao, J. KO, N. Choi, D. W. Lim, E. K. Lee, S. I. Chang and J. Choo, Lab Chip, 2013, 13, 260-266.
24. M. P. Cecchini, A. Wiener, V. A. Turek, H. Chon, S. Lee, A. P. Ivanov, D. W. McComb, J. Choo, T. Albrecht, S. A. Maier and J. B. Edel, Nano Lett., 2013, 13, 4602-4609.
25. Y. Zhu and Q. Fang, Anal. Chim. Acta, 2013, 787, 24-35.
26. S. Liu, Y. Gu, R. B. Le Roux, S. M. Mattehews, D. Bratton, K. YunusA. C. Fisher and W. T. S. Huck, Lab Chip, 2008, 8, 1937-1942.
27. C. D. Syme, C. Martino, R. R. Yusyana, N. M. S. Sirimuthu and J. M. Cooper, Anal. Chem., 2012, 84, 1491-1495.
28. K. Kantarovich, I. Tsarfati, L. A. Gheber, K. Haupt and I. Bar, Biosens. Bioelectron., 2010, 26, 809-814.
29. G. Wang, C. Lim, L. Chen, H. Chon, J. Choo, J. Hong and A. J. deMello, Anal. Bioanal. Chem., 2009, 394, 1827-1832.
30. R. Gao, N. Choi, S. I. Chang, S. H., Kang, J. M. Song, S. I. Cho, D. W. Lim and J. Choo, Anal. Chim. Acta, 2010, 681, 87-91.
31. Q. Zhou, J. Mao, J. Xiao and G. Xie, Anal. Methods, 2010, 2, 1063-1068.
32. Z. Yao, X. Hu, W. Ma, X. Chen, L. Zhang, J. Yu, Y. Zhao and H. C. Wu, Analyst, 2013, 138, 5572-5575.
33. Drinking Water Health Advisory: Pesticides, US Environmental Protection Agency, Lewis, Chelsea, MI, 1989.
34. N. Leopold and B. Lendl, J Phys Chem B, 2003, 107, 5723-5727.
35. M. L. Roldan, S. Sanchez-Cortes, J. V. Garcia-Ramos and C. Domingo, Phys. Chem. Chem. Phys., 2012, 14, 4935-4941.
36. M. R. Lopez-Ramirez, L. Guerrini, J. V. Garcia-Ramos and S. Sanchez-Cortes, Vib. Spectrosc., 2008, 48, 58-64.
37. A. Walter, A. März, W. Schumacher, P. Rösch and J. Popp, Lab Chip, 2011, 11,

1013-1021.

38. A. März, B. Mönch, P. Rösch, M. Kiehntopf, T. Henkel and J. Popp, Anal. Bioanal. Chem., 2011, 400, 2755-2761.

Figure Legends

Fig. 1 (a) Schematic illustration of an integrated microdroplet channel for SERS detection of DQ. The channel is composed of two compartments. The first is the synthetic section for AgNPs synthesis (i), and the second is for droplet merging and SERS analysis (ii). (b) Expanded view of the first compartment (i): nucleation of silver ions and large silver nanoparticles. (c) Expanded view of the second compartment (ii): intersection for droplet (AgNPs and DQ) merging and SERS detection. (d) Optical images of the entire microdroplet channel filled with two different colors (red and blue) of ink.

Fig. 2 (a) Photograph of the microdroplet channel and three laser focusing points for SERS measurements, and (b) corresponding SERS spectra for (i) carrier oil, (ii) 2×10^{-5} M DQ solution, and (iii) 2×10^{-5} M DQ solution with silver colloids.

Fig. 3 (a) Sequential merging process between two droplets (AgNPs and DQ molecules), and six different channel positions for SERS measurements in the second channel compartment. (b) Relative SERS intensities at 1579 cm^{-1} along the channel position.

Fig. 4 Concentration-dependent SERS spectra of DQ in the integrated microdroplet channel. The concentrations ranged from 5×10^{-6} to 5×10^{-9} M. (b) Variation of DQ peak intensity at 1579 cm^{-1} of SERS spectra as a function of DQ concentration. Correlation coefficient, R^2 = 0.995; error bars indicate the standard deviations of three measurements.

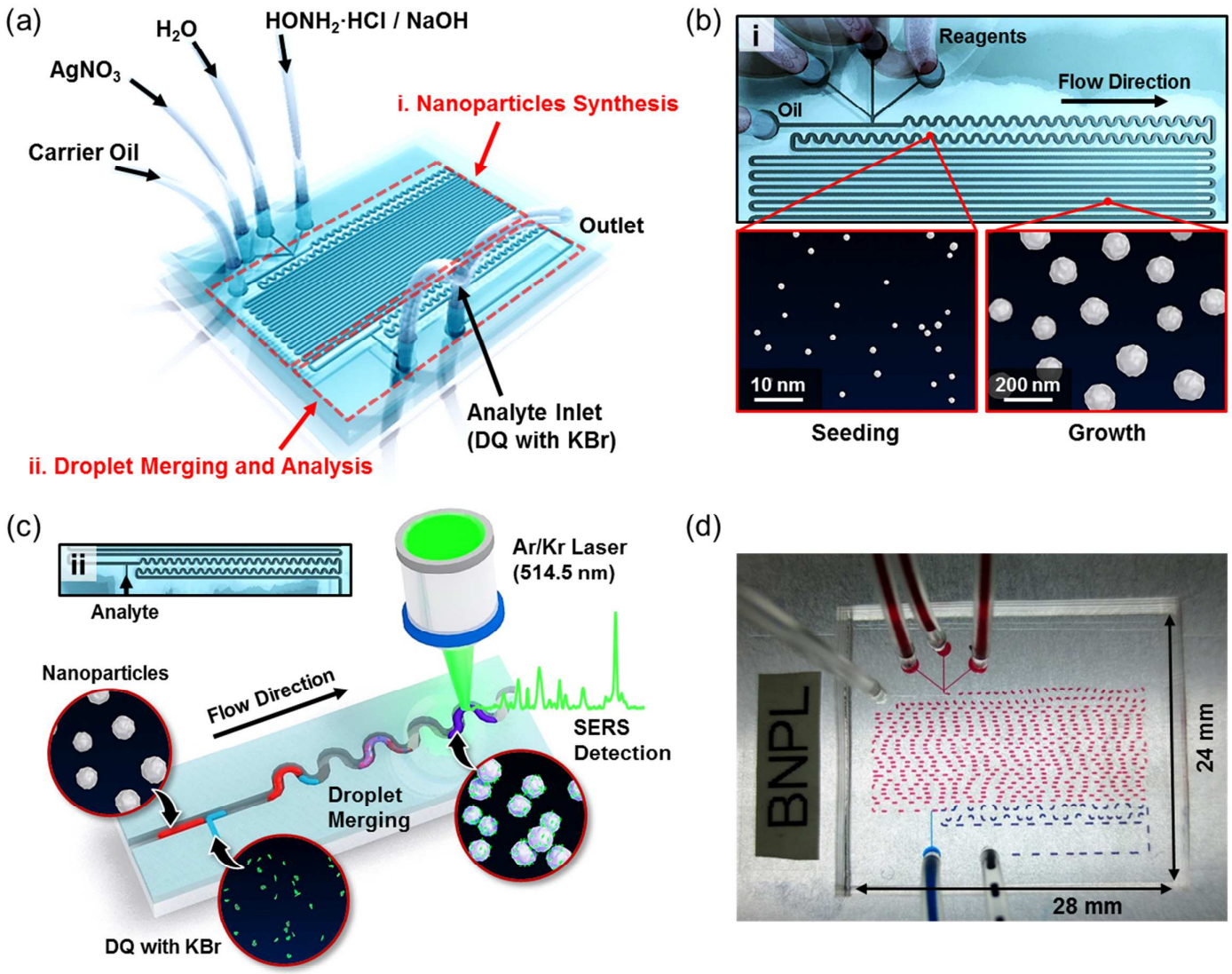

Figure 1

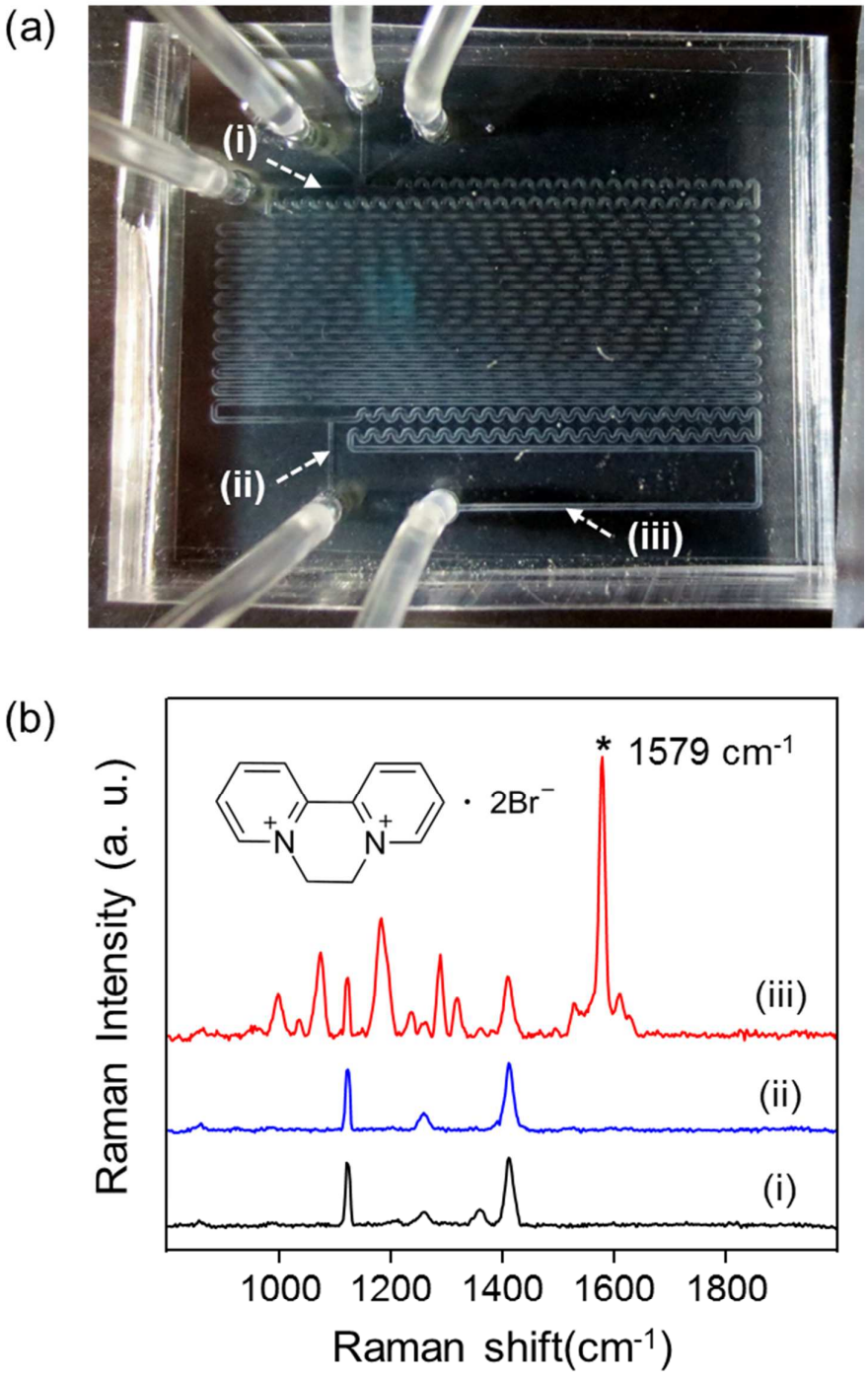

Figure 2

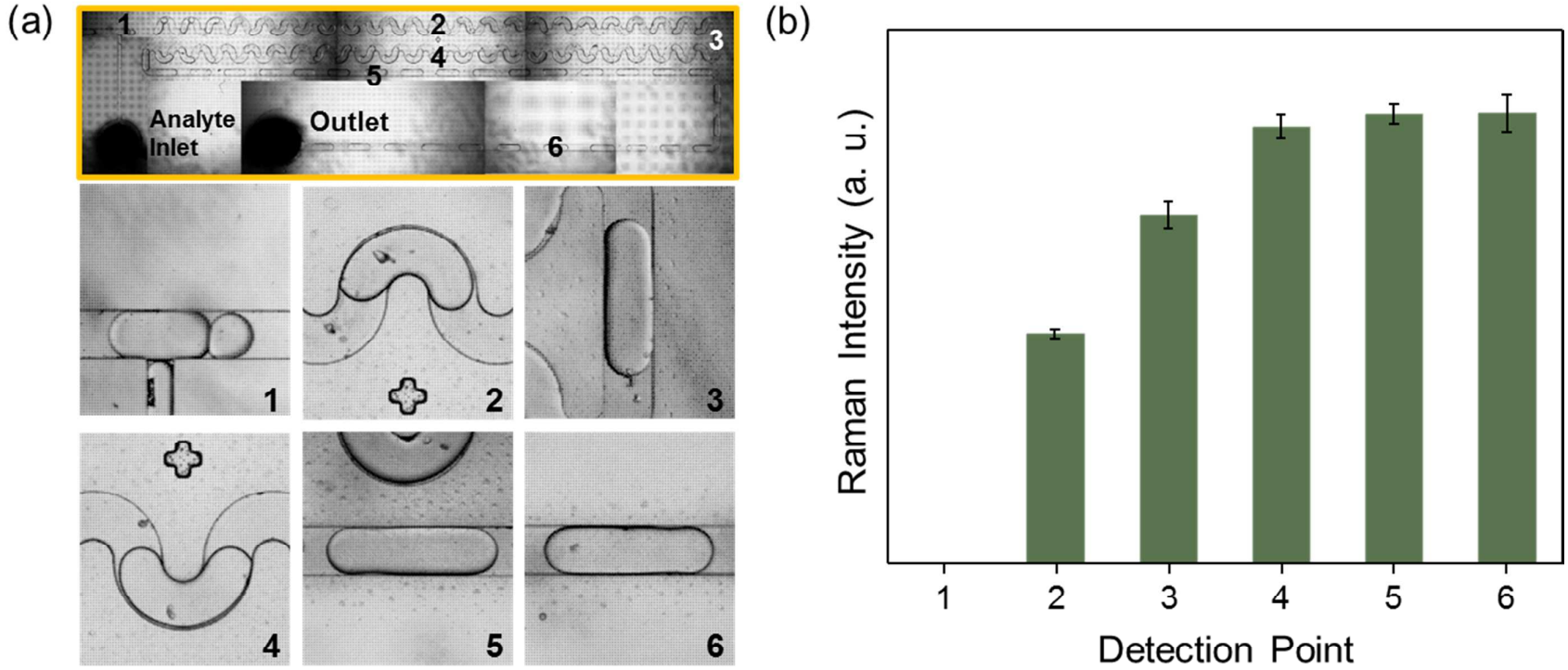

Figure 3

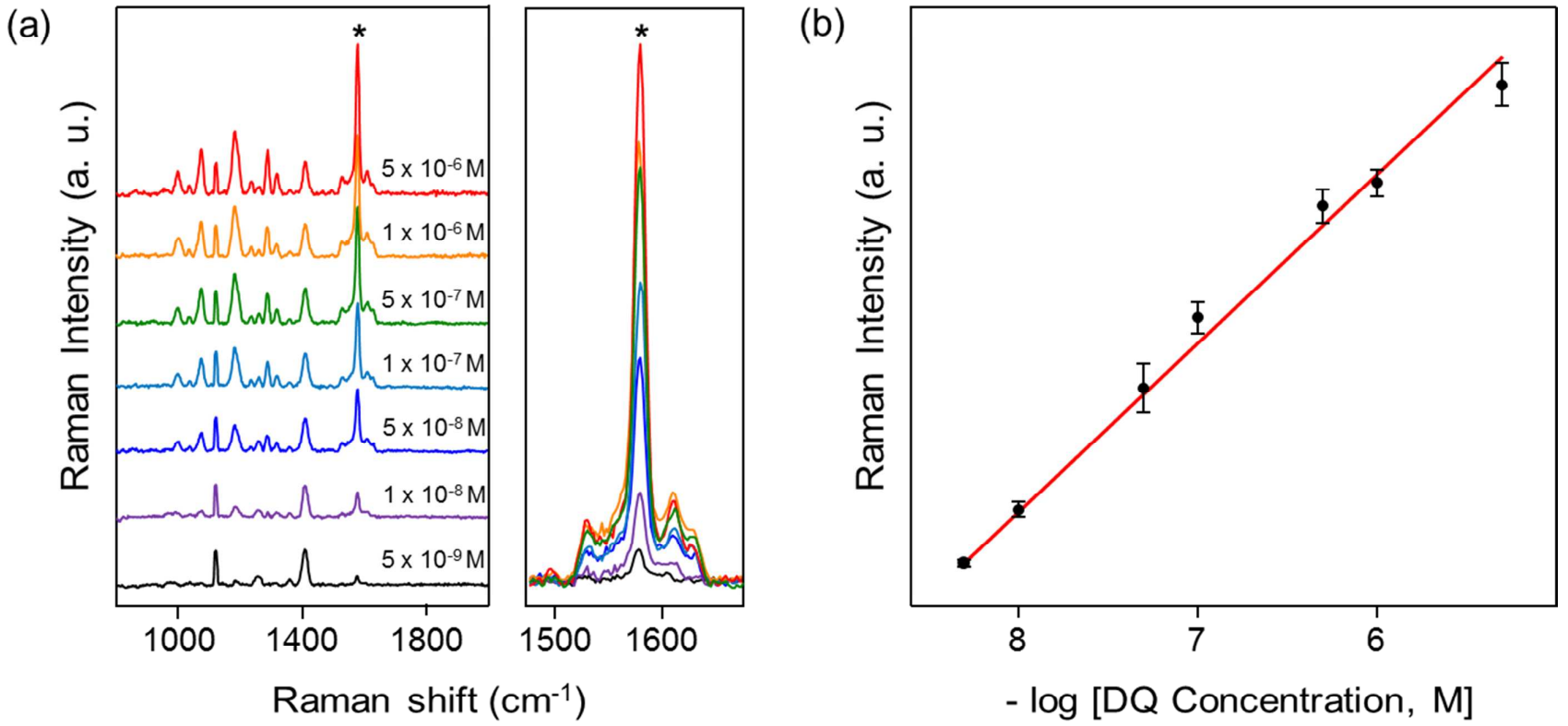

Figure 4